Materials Letters 140 (2015) 162–165

Contents lists available at ScienceDirect

Materials Letters

journal homepage: www.elsevier.com/locate/matlet

Visualizing reactive oxygen species inside cancer cells after stimulation with polycyclic aromatic hydrocarbon *via* spontaneous formation of Au nanoclusters

Chalermchai Pilapong [a,*,1], Siwatt Pongpiajun [b], Samlee Mankhetkorn [a]

[a] *Center of Excellence for Molecular Imaging (CEMI), Department of Radiologic Technology, Faculty of Associated Medical Science, Chiang Mai University, Chiang Mai 50200, Thailand*

[b] *NIDA Center for Research & Development of Disaster Prevention & Management, School of Social and Environmental Development, National Institute of Development Administration (NIDA), Bangkok 10240, Thailand*

ARTICLE INFO

Article history:
Received 14 July 2014
Accepted 30 October 2014
Available online 7 November 2014

Keywords:
Gold nanocluster
Reactive oxygen species
Chloroauric acid

ABSTRACT

This research was designed to visualize cellular response – in particular the generation of intracellular ROS – to stimulation by polycyclic aromatic hydrocarbon (PAH). We used chloroauric acid ($HAuCl_4$) as a molecular probe for visualizing intracellular ROS generated by the stimulation of benzo[a]pyrene (BaP). The chloroauric acid undergoes a spontaneous reduction reaction, assisted by the intracellular ROS, into gold nanoclusters (AuNCs). As a result, we can visualize the ROS *via* optical imaging technique. According to MTT assay, the chloroauric acid exhibited good biocompatibility. The AuNCs produced in the cells were approximately 2–3 nm in diameter with a green fluorescent property. Cellular imaging showed that BaP induced the formation of AuNCs within the cells, leading to a high relative cellular fluorescent intensity with a considerable extent of scatter light. Thus, this probe is an efficient molecular imaging probe for visualizing intracellular ROS.

1. Introduction

Polycyclic aromatic hydrocarbons (PAHs) can cause cancer, heritable genetic damage and sensitization by skin contact, among other health issues. Exposure to PAHs may lead cells, as an early-stage response, to overproduce intracellular reactive oxygen species (ROS), causing oxidative stress [1–3]. Generally, abnormal overproduction of intracellular ROS is closely associated with various pathological processes, including cancer, cardiovascular disease and neurological disorders [4]. Various fluorescent probes for detecting ROS have been developed, including small molecule-based and nanoparticle-based probes. However, use of these probes is limited by their toxicity and they cannot be used for spontaneous imaging. Moreover, some probes cannot be used to spontaneously monitor intracellular ROS induced by a highly toxic reagent [5–11].

To overcome these limitations, we build on the concept that metal nanoclusters and nanoparticles can be simultaneously synthesized by using various kinds of reducing agents – such as a highly toxic agent ($NaBH_4$) [12], biomolecules (RNase A, ovalbumin) [13,14] and ROS compounds [15,16] – to form fluorescent metal nanoclusters in order to visualize intracellular ROS in hepatocellular carcinoma cells after being stimulated with PAH compounds (benzo[a]pyrene, BaP). We postulated that BaP molecules enter cells and stimulate them to produce intracellular ROS. In the presence of chloroauric salt ($HAuCl_4$) within the cell, $HAuCl_4$ can undergo a rapid and efficient spontaneous reduction by intracellular ROS into fluorescent gold nanoclusters. Thus, we could spontaneously visualize intracellular ROS, induced by polycyclic aromatic hydrocarbon, *via* optical imaging technique.

2. Experimental details

Physical characterization: Size of AuNCs, obtained from the cells by a repetitive freeze–thaw method, was measured with a field-emission transmission electron microscope (TEM, JEOL JEM-2100).

* Corresponding author at: Center of Excellence for Molecular Imaging (CEMI), Department of Radiologic Technology, Faculty of Associated Medical Science, Chiang Mai University, Chiang Mai 50200, Thailand. Tel.: +66 53 94 9306; fax: +66 53 21 3218.
E-mail address: chalermchai.pilapong@cmu.ac.th (C. Pilapong).
[1] Post-Doctoral Research Fellow, National Institute Development Administration (NIDA), Bangkok 10240, Thailand.

http://dx.doi.org/10.1016/j.matlet.2014.10.157
0167-577X/

Fluorescence and excitation spectra of AuNCs were determined with an LS55 luminescence spectrometer. UV–vis absorbance was measured on an Agilent 8453 UV–visible spectrometer.

Cell viability: HepG2 cells (hepatocellular carcinoma cells) or HepG2.2.15 cells (hepatitis B virus infected hepatocellular carcinoma cells) were trypsinized and resuspended in DMEM. The cells were seeded in a 24-well plate at a density of 5×10^4 cells/mL and incubated overnight at 37 °C in 5% CO_2 atmosphere. After washing, DMEM containing $HAuCl_4$ was loaded in each well with final concentrations of 0, 0.1, 1, 10, 100 and 1000 μM. After 48 h incubation, the culture medium was discarded and the cells were washed twice with PBS buffer and further incubated with 200 μL of solution containing 5 mg MTT/mL phosphate-buffered saline at 37 °C for 4 h. The MTT solution was removed and the intracellular formazan cystals were dissolved with 500 μL DMSO for 15 min at 37 °C. The absorbance of formazan solution was measured through spectroscopy at 570 nm with DMSO as blank.

Cellular imaging study: The trypsinized cells were seeded at a density of 5×10^4 cells/well and incubated in DMEM at 37 °C in 5% CO_2. After 24 h incubation, the cells were washed twice with PBS buffer and further incubated with the culture medium containing BaP alone, $HAuCl_4$ alone or co-incubation of BaP and $HAuCl_4$. After 24 h incubation, the cells were washed with PBS and observed under a Leica DMI 4000B microscope.

3. Results and discussion

TEM and fluorescence analysis were used to confirm the formation of AuNCs within the cells. Figs. 1a and S1 show, respectively, the TEM image and EDS spectrum of AuNCs produced inside HepG2 cells after incubation with the appropriate amount of $HAuCl_4$ and BaP for 24 h. The AuNCs were measured as approximately 2–3 nm without any impurity elements. The HRTEM image (Fig. 1a(inset)) reveals a lattice fringe with a spacing of ~2.4 Å, which is in good agreement with the lattice spacing in the (111) planes of face centered cubic gold. The AuNCs exhibited an optimum excitation wavelength of 450 nm and a maximum emission wavelength of 525 nm (Fig. 1b); the origin of PL band centered at ~530 nm is ascribed to the presence of Au_{13} species, which act as main emitters inside the cells [17]. These results confirmed that cells stimulated with BaP spontaneously produced intracellular fluorescent AuNCs. The formation of fluorescent AuNCs inside the cells might be due to a reduction of Au (III) by competing with reduction of dioxygen and/or the intracellular ROS e.g., superoxide anion ($O_2\bullet$), and subsequent surface capping by specific ligands inside the cells [18,19]. However, the formation mechanism is still unclear, and beyond the scope of this study.

To demonstrate a potential use of $HAuCl_4$ as a biocompatible ROS imaging probe, we initially tested the cytotoxicity of $HAuCl_4$ toward HepG2 and HepG2.2.15 cells by using MTT assay. As shown in Fig. 2, no toxicity was observed in the cells incubated with 0–100 μM of $HAuCl_4$, indicating this probe's good biocompatibility. At an even higher concentration of $HAuCl_4$ (1000 μM), the cellular viability remained approximately 80%. These MTT assays indicated that $HAuCl_4$ has low cytotoxicity.

To show the feasibility of $HAuCl_4$ as a spontaneous fluorescent imaging probe for visualizing intracellular ROS produced inside cancer cells after BaP stimulation, the HepG2 cells were incubated with the culture medium containing BaP alone, $HAuCl_4$ alone or co-incubation of BaP and $HAuCl_4$. After 24 h incubation, the cells were washed with PBS several times and observed under a Leica DMI 4000B fluorescence microscope. As shown in Fig. 3, a higher relative cellular green fluorescent intensity was observed in the HepG2 cells incubated with both $HAuCl_4$ and BaP (Fig. 3e), and even higher as the concentration of BaP was increased (Figs. 3f and S2). The higher fluorescent intensity demonstrated that BaP induced the formation of AuNCs *via* a spontaneous reduction reaction assisted by the intracellular ROS. This confirms that $HAuCl_4$ is an efficient molecular imaging probe for inflammation induced by a highly toxic compound (e.g., PAHs). Furthermore, we observed a strong green fluorescence near cell membranes, indicating an active location for AuNCs formation inside the cells. This result accords well with previous reports, which indicated

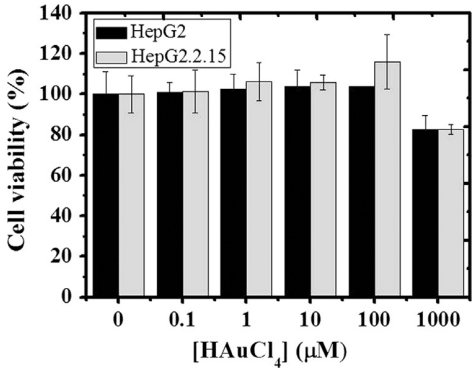

Fig. 2. Cell viability determined by MTT assay in HepG2 and HepG2.2.15 cells.

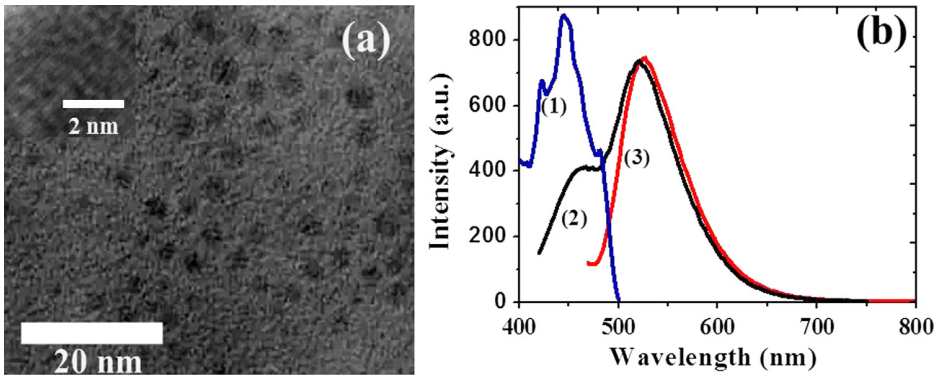

Fig. 1. (a) TEM image of AuNCs obtained from the cells by a repetitive freeze–thaw method (scale bar =20 nm), (b) fluorescent spectra of the AuNCs obtained using 400 nm excitation wavelength (2) and 450 excitation wavelength (3) with their excitation spectra (1).

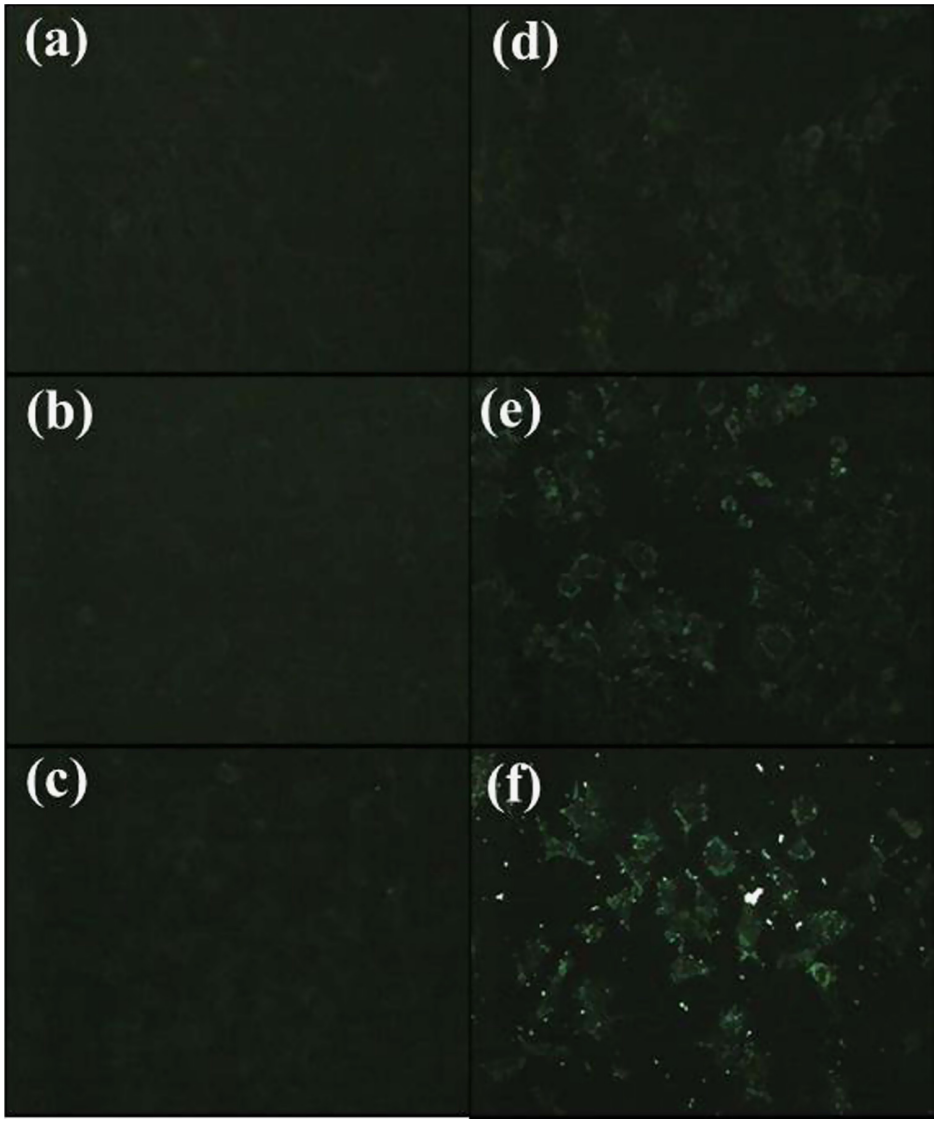

Fig. 3. Fluorescence images of untreated HepG2 cells (a), 0.1 μM BaP treated cells (b), 1 μM BaP treated cells (c), 0.5 mM $HAuCl_4$ treated cells (d), 0.5 mM $HAuCl_4$+0.1 μM BaP treated cells (e), and 0.5 mM $HAuCl_4$+1 μM BaP treated cells (f).

important enzymatic pools near cell membranes [20,21]. While the probe was suitable for visualizing the ROS pool in cancer cells, it was not specific to individual ROS. In addition to fluorescence imaging, dark field imaging is normally used for analyzing biological samples containing scattered nanomaterials e.g., gold nanoparticles. Dark field images of HepG2 cells (Fig. 4) showed that a higher accumulation of AuNCs were observed in the cells treated with both $HAuCl_4$ and BaP. These results are in good accordance with those observed in fluorescence imaging. Therefore, we can simultaneously visualize intracellular ROS *via* both fluorescence and dark field imaging techniques by using a biocompatible $HAuCl_4$ as molecular probe.

The same strategy was also applied for HepG2.2.15 cells. As shown in Fig. S2, a much higher fluorescent intensity was observed in both HepG2 and HepG2.2.15 cells co-incubated with $HAuCl_4$ and BaP, compared to $HAuCl_4$ alone. This is also due to an over-generated intracellular ROS after BaP stimulation, leading to a high relative cellular fluorescent intensity. This confirms that our molecular probe can visualize ROS inside both HepG2 and HepG2.2.15 cells after being stimulated by BaP.

4. Conclusion

We utilized $HAuCl_4$ as a molecular probe for visualizing ROS inside cancer cells after stimulation with a highly toxic agent (benzo[a]pyrene, BaP). The intracellular ROS reduces $HAuCl_4$ into fluorescent AuNCs. The presence of AuNCs inside the cells can be confirmed by TEM and fluorescent spectrum. According to cellular fluorescent and dark field imaging, BaP induced the formation of AuNCs inside the cancer cells, observed as a high relative cellular fluorescent intensity and scattered light, respectively. Thus, this molecular probe can be used to study cellular response (ROS generation) to stimulation by a highly toxic polycyclic aromatic hydrocarbon, *via* optical imaging technique.

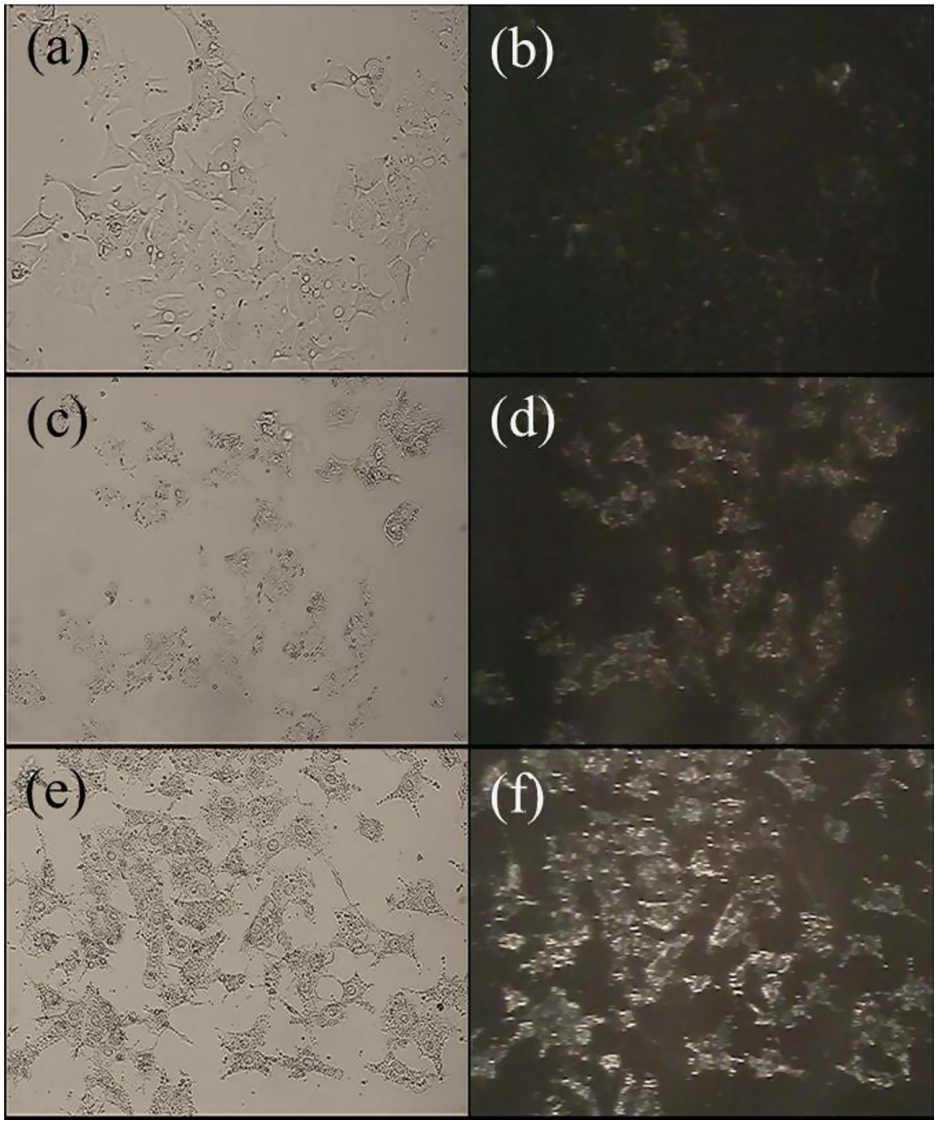

Fig.4. Bright field and dark field images of untreated HepG2 cells (a), 0.5 mM $HAuCl_4$ treated cells (b) and 0.5 mM $HAuCl_4$+1 μM BaP treated cells (c).

Acknowledgments

We would like to thank National Institute Development Administration (NIDA), Thailand, for providing financial support through Post-Doctoral Research Fellowship.

Appendix A. Supporting information

Supplementary data associated with this article can be found in the online version at http://dx.doi.org/10.1016/j.matlet.2014.10.157.

References

[1] Wilk A, Waligórski P, Lassak A, Vashistha H, Lirette D, Tate D, et al. J Cell Physiol 2013;228:2127–38.
[2] Chung SW, Chung HY, Toriba A, Kameda T, Tang N, Kizu R, et al. Toxicol Sci 2007;95:348–55.
[3] Song MK, Kim YJ, Song M, Choi HS, Park YK, Ryu JC. Cancer Sci 2011;102:1636–44.
[4] Medzhitov R. Nature 2008;454:428–35.
[5] Beltran-Huarac J, Tomar MS, Singh SP, Perales O, Rivera L, Peña S. NSTI-Nanotech 2010;3:405–8.
[6] Soh N. Anal Bioanal Chem 2006;386:532–43.
[7] Hempel SL, Buettner GR, O'Malley YQ, Wessels DA, Flaherty DM. Free Radic Biol Med 1999;27:146–59.
[8] Miller EW, Tulyathan O, Isacoff EY, Chang CJ. Nat Chem Biol 2007;3:263–7.
[9] Lee D, Khaja S, Velasquez-Castano JC, Dasari M, Sun C, Petros J, et al. Nat Mater 2007;6:765–9.
[10] Pu K, Shuhendler AJ, Rao J. Angew Chem Int Ed 2013;52:10325–9.
[11] Chen T, Hu Y, Cen Y, Chu X, Lu Y. J Am Chem Soc 2013;135:11595–602.
[12] Yin J, He X, Wang K, Qing Z, Wu X, Shi H, et al. Nanoscale 2012;4:110–2.
[13] Qiao J, Mu X, Qi L, Deng J, Mao L. Chem Commun (Camb) 2013;49:8030–2.
[14] Kong Y, Chen J, Gao F, Brydson R, Johnson B, Heath G, et al. Nanoscale 2013;5:1009–17.
[15] Li Q, Lu B, Zhang L, Lu C. J Mater Chem 2012;22:13564–70.
[16] Liu X, Xu H, Xia H, Wang D. Langmuir 2012;28:13720–6.
[17] Chattoraj S, Bhattacharyya K. J Phys Chem C 2014;118:22339–46.
[18] Turrens JF. J Physiol 2003;552:335–44.
[19] Wang J, Zhang G, Li Q, Jiang H, Liu C, Amatore C, et al. Sci Rep 2013;3:1157.
[20] Amatore C, Arbault S, Guile M, Guile M. Chem Rev 2008;108:2585–621.
[21] Wiseman H, Halliwell B. Biochem J 1996;313:17–29.